

# Non-LBL Assembly and Encapsulation Uses of Nanoparticle-Shelled Hollow Spheres

Gautam C. Kini, Sibani L. Biswal, and Michael S. Wong

**Abstract** Nanoparticles (NPs, diameter range of 1–100 nm) can have size-dependent physical and electronic properties that are useful in a variety of applications. Arranging them into hollow shells introduces the additional functionalities of encapsulation, storage, and controlled release that the constituent NPs do not have. This chapter examines recent developments in the synthesis routes and properties of hollow spheres formed out of NPs. Synthesis approaches reviewed here are recent developments in the electrostatics-based tandem assembly and interfacial stabilization routes to the formation of NP-shelled structures. Distinct from the well-established layer-by-layer (LBL) synthesis approach, the former route leads to NP/polymer composite hollow spheres that are potentially useful in medical therapy, catalysis, and encapsulation applications. The latter route is based on interfacial activity and stabilization by NPs with amphiphilic properties, to generate materials like colloidosomes, Pickering emulsions, and foams. The varied types of NP shells can have unique materials properties that are not found in the NP building blocks, or in polymer-based, surfactant-based, or LBL-assembled capsules.

**Keywords** Hollow spheres · Nanoparticles · Layer-by-layer assembly · Tandem assembly · Nanoparticle assembled capsule · Interfacial stabilization · Particle stabilized emulsion

---

G.C. Kini and S.L. Biswal  
Department of Chemical and Biomolecular Engineering, Rice University, Houston,  
TX, 77005, USA  
e-mail: [gck1@rice.edu](mailto:gck1@rice.edu); [biswal@rice.edu](mailto:biswal@rice.edu)

M.S. Wong (✉)  
Department of Chemical and Biomolecular Engineering, Rice University, Houston,  
TX, 77005, USA  
and  
Department of Chemistry, Rice University, Houston, TX, 77005, USA  
e-mail: [mwong@rice.edu](mailto:mwong@rice.edu)

## Contents

1	Introduction
2	Hollow Spheres from Electrostatic Assembly of Nanoparticles Through Tandem Assembly
2.1	Current Methods
2.2	Preparation of Two-Nanoparticle-Type Hollow Spheres
2.3	Preparation of One-Nanoparticle-Type Hollow Spheres
2.4	Applications and Properties of Tandem-Assembled Capsules
3	Interfacial Stabilization and Other Approaches to the Assembly of Nanoparticle-Shelled Hollow Structures as Emulsions and Foams
4	Conclusions and Future Work
	References

## Abbreviations

Cys	Cysteine
E	Energy of attachment
EDTA	Tetrasodium ethylenediamine tetraacetate
FDA	Food and Drug Administration
ICG	Indocyanine green
$k$	Boltzmann's constant
LBL	Layer-by-layer
Lys	Lysine
NAC	Nanoparticle assembled capsule
NIR	Near-infrared
NP	Nanoparticle
O/W	Oil-in-water
PAA	Poly(acrylic acid)
PAH	Poly(allylamine hydrochloride)
PE	Polyelectrolyte
PLL	Poly-L-lysine
QD	Quantum dot
$R$	$R$ ratio, defined as the total negative charge from a multivalent anion divided by the total positive charge from the polymer
$r$	Particle radius
SEM	Scanning electron microscope
$T$	Temperature
TEM	Transmission electron microscope
TGA	Thermogravimetric analysis
W/O	Water-in-oil

## 1 Introduction

The study of colloids and interfaces has resulted in identification of key short-range interactions and systematized understanding of colloidal interactions [1–5]. One of the tangibles that has emerged is the creation of assemblies with precision down to nanoscale levels, which hold promise as next-generation devices in technology-driven applications. Ranging from traditional areas such as agriculture and mining to the latest in cutting-edge fields that include nanotechnology and biotechnology, it is apparent that approaches to the control and creation of assemblies using building blocks with custom-designed functionalities are essential to sustain advancements in technology [6–20].

A class of colloidal assemblies that evokes interest in its synthesis approaches and physicochemical properties are “hollow spheres” or “capsules” [21]. Hollow spheres are discrete volume closures that have a well-defined boundary separating the interior from the bulk external environment [8, 22]. Popular routes for the synthesis of hollow spheres can be categorized into self-assembly, chemical reactions, sequential electrostatic assembly, and interfacial stabilization approaches [9, 13, 23–40].

The shell interior (hollow region) can be empty or filled (with a liquid but not a solid). The shell boundary is typically constituted of materials such as particles, polymers, charged polymers or polyelectrolytes (PEs), low-molecular-weight molecules such as enzymes, or their combinations [41]. These structures find wide applications in fields such as encapsulation, targeted and controlled drug delivery, personal care, biosensing, diagnostics, catalysis and paints [13, 32, 42, 43].

This review examines recent developments in the synthesis routes and properties of hollow spheres formed out of nanoparticles (NPs, diameter range 1–100 nm). Of specific interest to this review are cases where NPs (metal, metal oxide, and semiconductor compositions) constitute a part of the coating and can impart to the structures their optical, magnetic, and catalytic properties. To tailor next-generation devices with custom-built functionalities, methods for assembling NPs into controlled patterns and architectures are required and have resulted in areas of active research [7, 10, 44–46]. There are many excellent reviews that consider NPs as building blocks and describe methodologies to create functional NP assemblies [6, 47–53]. These include accounts that describe strategies and mechanisms for NP assemblies in one, two and three dimensions (1D, 2D and 3D), like wires, dyads, triads, rods, rings, clusters, strings, and spheres [54–64].

No review exists so far that examines the newest methodologies [apart from the popular layer-by-layer (LBL) assembly route] for forming hollow spheres or capsules where the shell is comprised of NPs, or describes the resultant properties of such assemblies. This is an area of immense significance as the utility of NPs in forming shell boundaries offers specific advantages over those formed by microparticles or polymers. Advantages include accurate control over shell thickness, resolvable to nanometer scales, and synergistic benefits gained through NP-exhibited “size-quantization effects” that give the system a host of new mechanical, optical, electrical, magnetic, and catalytic properties. Further, individual

NPs can be functionalized with chemical moieties (amino or mercapto groups or DNA), making them capable of binding to specific target sites through well-known amino or thio complexation chemistry or through Watson–Crick base pair interactions with DNA oligonucleotides. Thus, “smart” NP-shelled hollow spheres that are responsive to external triggers (pH, ionic strength, laser sources etc.) can be prepared [65–68]. Section 2 focuses on the electrostatic assembly approach to the synthesis of NP-shelled hollow spheres, specifically the NP–polymer tandem assembly route. Section 3 concerns interfacial stabilization methods for assembly of NP-shelled hollow spheres. Distinctions in properties that emerge from NP-shelled hollow spheres in comparison to their non-NP analogues will be highlighted [5, 19, 46, 69–73].

## 2 Hollow Spheres from Electrostatic Assembly of Nanoparticles Through Tandem Assembly

### 2.1 Current Methods

The use of colloidal templates has emerged as an elegant approach for the assembly of NPs into hollow spheres. Typically, hollow sphere synthesis begins by coating the core template with materials such as polymers and NPs using electrostatics or van der Waals attractive forces in conjunction with a reactive precursor. This is followed by a polymerization chemical reaction to form the shell. Removal of the core template by chemical dissolution or calcination results in hollow spheres [21, 74]. The term often used to describe this method – “sacrificial core templating” – can be somewhat misleading because it implies that other approaches do not involve the use and removal of a core template to form hollow spheres. To avoid any confusion, here we use the term “covalent assembly” in place of “sacrificial core templating” to distinguish its use of a reactive precursor to covalently bind the shell together.

An alternate route to assembly of nanoparticles as hollow spheres that does not require a polymerization reaction step is sequential electrostatic assembly. Electrostatic-mediated multilayer assembly of charged particles was first demonstrated by R. Iler on planar surfaces, wherein he established the proof-of-principle to deposit particles sequentially onto solid substrates [25]. Decher advanced this scheme by assembling alternately charged PEs (e.g., polycations and polyanions) onto solid supports. Ever since, this scheme has been used to form capsules by sequential electrostatic deposition of single or multiple coatings of materials on pre-formed colloidal templates and subsequent removal of the template by calcination or solvent dissolution. This constitutes the LBL method for assembly of hollow spheres.

Figure 1 depicts LBL assembly of hollow spheres. The first step involves surface modification of pre-formed solid colloidal templates (most commonly negatively charged) by depositing a layer of oppositely charged PE (here positive) through attractive electrostatic interactions. This step deposits the first layer of surface

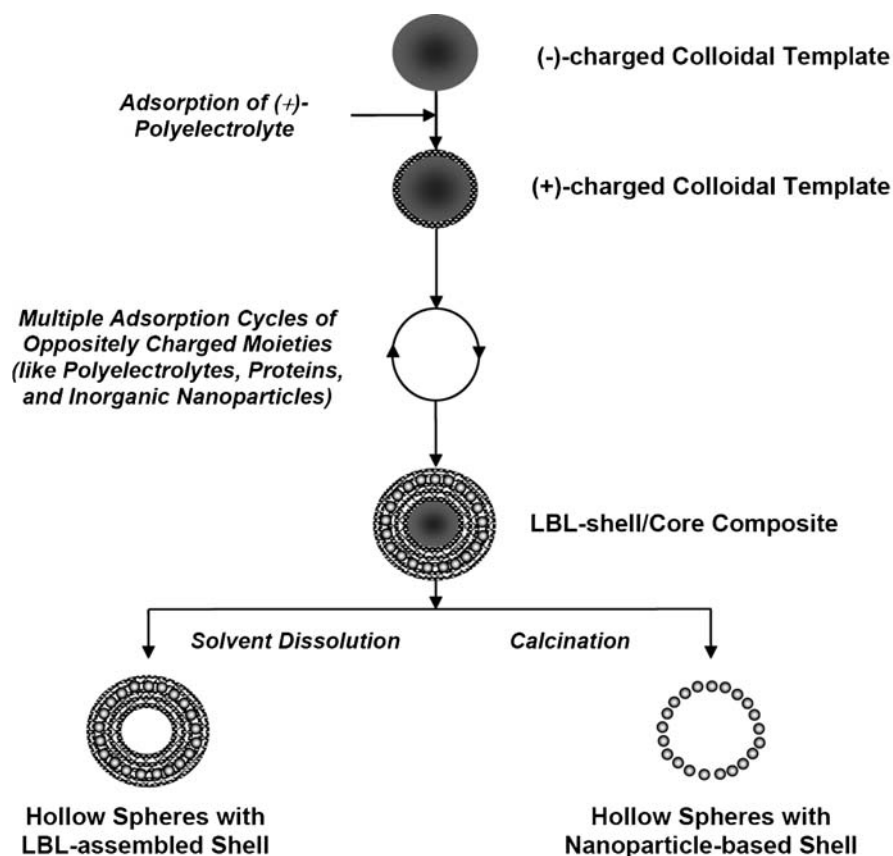


**Fig. 1** LBL assembly routes for formation of NP-shelled inorganic capsules

coating and results in charge reversal of the ensemble (in this case, positive). Following the first cycle of deposition, unadsorbed material is removed by centrifugation, wash, and filtration steps. Different combinations of charged moieties can be added, including PEs, proteins in the form of enzymes, organic dyes, and NPs. At the end of each cycle of deposition, unadsorbed material is removed by procedures described previously, and the process is repeated. Multiple repetitions lead to multi-layered composite structures, with each closed-shell layer made of a given charged moiety.

Capsules can then be formed by either a calcination or a dissolution step to create hollow structures. Calcination (typically carried out at a temperature of  $\sim 450^\circ\text{C}$ ) removes all the organic constituents (like the colloidal template core and the organic shell-forming moieties), leaving the constituent inorganic NPs slightly sintered to form robust shell walls. Solvent dissolution of the core material yields hollow spheres, which retain all the shell constituents. The LBL approach is thus a versatile route for creation of NP-shelled hollow spheres. Extensive reviews on forming

functional capsules by the LBL methods have been provided by Caruso and others and are beyond the scope of this chapter [13, 29, 30, 75].

A disadvantage common to both covalent and LBL assembly routes is the multiple steps involved in materials assembly. Automation of these layering steps provides an excellent approach to address this issue and leads to LBL-based manufacturing capabilities [76]. Also of concern are requirements of an incineration or solvent dissolution step to remove the core in order to form hollow spheres. It is a non-trivial challenge to selectively remove the inner core without degrading the shell properties and affecting structural integrity [13, 29, 30, 75]. Recent work demonstrates that liquid colloidal templates in the form of surfactant-stabilized liquid crystal droplets can be used successfully in the LBL assembly of capsules [77–79]. Such liquid droplets can further be used in continuous-flow production of LBL-assembled capsules via microfluidic technology.

Another recent development features the in situ formation of liquid colloidal templates. The assembly of NPs at the periphery of these templates is driven by electrostatics, resulting in the formation of robust NP-shelled hollow spheres, originally termed “nanoparticle-assembled capsules” (NACs). This scheme is called “tandem assembly”, “nanoparticle–polymer tandem assembly”, or “polymer-aggregate templating” and presents an alternate, simple and non-destructive route for formation of NP-shelled hollow spheres [6, 32–35, 40, 80, 81].

When comparing the time scales of transport of material to the hollow capsule interiors, the efficiency of encapsulation arising from assembly schemes featuring in situ encapsulation should be higher than for hollow structures formed by core-shell dissolution. Time requirements should be higher for hollow capsules contacted in a solution of material to be encapsulated, particularly when material transport is based on kinetically driven diffusion or absorption processes, as compared to an in situ encapsulation scheme. In the case of material transport governed by a thermodynamic phenomenon such as partitioning, the equilibrium quantity of material that needs to be transported across the shell will be dependent on the partition coefficient of the shell with respect to the material to be encapsulated [13, 32–35, 80–83].

## ***2.2 Preparation of Two-Nanoparticle-Type Hollow Spheres***

The origin to tandem assembly can be traced to the investigations by Stucky and coworkers on cooperative charge-based assembly of lysine (Lys)-cysteine (Cys) diblock copolypeptides with SiO<sub>2</sub> and Au NPs to result in robust hollow spheres. Diblock copolypeptides containing amphiphilic groups (hydrophilic Lys, pK<sub>a</sub>~9, hydrophobic Cys, pK<sub>a</sub>~8), upon reaction with Au NPs (diameter 10–12 nm), led to the formation of spherical aggregates of Au NPs (Fig. 2) [32]. On further reaction with SiO<sub>2</sub> NPs, micron-sized hollow spheres were seen to form. It is worthwhile re-emphasizing that aggregates emerge spontaneously and that the process is an electrostatically driven self-assembly process, which is different from entropy-driven molecular self-assembly schemes exhibited by surfactants, block copolymers, and vesicles.

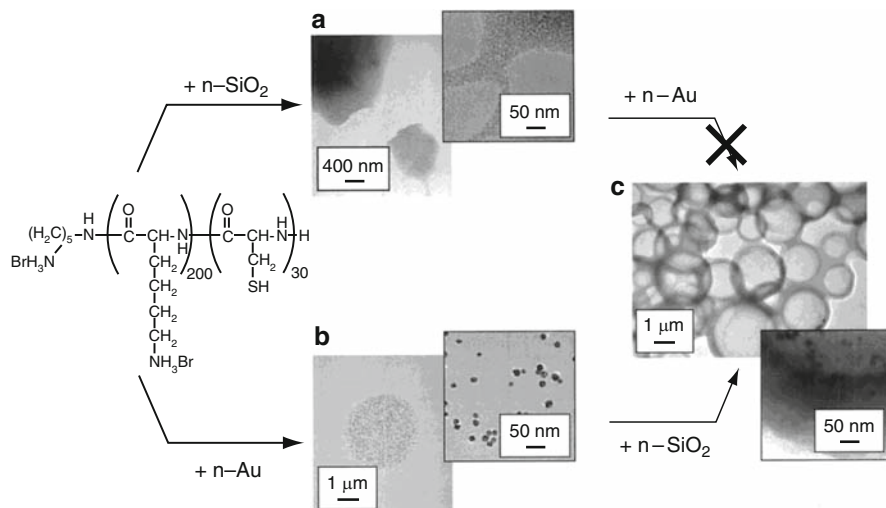


**Fig. 2** Formation of hollow spheres by tandem assembly of two NPs. **(a)** TEM images of  $\text{Lys}_{200}\text{Cys}_{30}/\text{n-SiO}_2$  precipitate. **(b)** TEM images of  $\text{Lys}_{200}\text{Cys}_{30}/\text{n-Au}$  precipitate. **(c)**  $\text{Lys}_{200}\text{Cys}_{30}/\text{n-Au}/\text{n-SiO}_2$  hollow spheres (*inset* shows areas of higher magnification). Structure in **(c)** is obtained only by adding  $\text{SiO}_2$  NPs to the  $\text{Lys}_{200}\text{Cys}_{30}/\text{n-Au}$  precipitate but is not formed when Au NPs are added to  $\text{Lys}_{200}\text{Cys}_{30}/\text{n-SiO}_2$  precipitate. Note: n-Au and n-SiO<sub>2</sub> represent Au and SiO<sub>2</sub> NPs, respectively. Reproduced from [32], with permission from the publisher

Noteworthy is the fact that hollow spheres did not form when diblock copolypeptides were reacted with SiO<sub>2</sub> NPs first and then with Au NPs, thus indicating the crucial role of Au NPs in forming hollow spheres by binding copolypeptide chains into submicron- and micron-sized aggregates. Walls of the hollow spheres that formed consisted of a distinct layer of Au followed by an outer layer of SiO<sub>2</sub> NPs with an average thickness of 250 nm. (as shown in Fig. 3). This indicates the flexibility and generic nature of the process, thus providing avenues for organization of multicompositional arrays of NPs. Also shown by a similar scheme was the formation of two-nanoparticle-type (2-NP) spheres from assembly of diblock copolypeptides poly-(L-Lys<sub>200</sub>-L-Cys<sub>30</sub>) with citrate-stabilized CdSe/CdS quantum dots (QDs) followed by a layer of SiO<sub>2</sub> NPs [84].

Stucky and coworkers furthered this work by studying citrate-stabilized CdSe QDs with single-block positively charged homopolymer PEs (poly-L-lysine, PLL) [33]. Macroscopic phase separation of initially water-soluble reactants were driven by molecular interactions between ligands on the inorganic phase (carboxylate groups of citric acid) and functional groups of the organic PEs (amino group on PLL), forming QD-PLL “vesicle”-like intermediates. The as-assembled QD NP vesicles collapsed on drying, but after addition of SiO<sub>2</sub> NPs to the reaction mixture, stable 3D hollow spheres formed with distinct localization of the two NP types. QDs were located at the interior, whereas SiO<sub>2</sub> NPs occupied the exterior of the shell wall, similar to the Au NP/SiO<sub>2</sub> NP/diblock copolypeptide capsules.

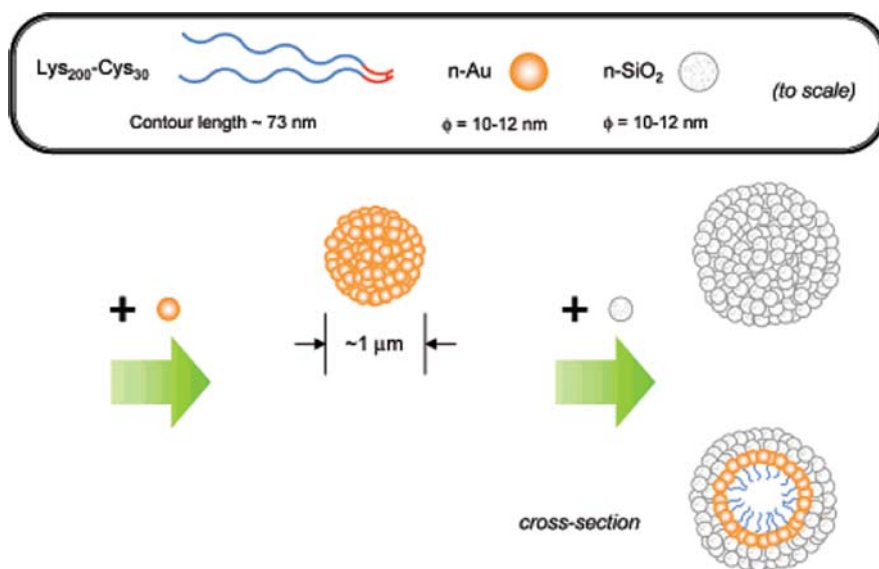


**Fig. 3** Hierarchical self-assembly of gold and silica NPs (n-Au and n-SiO<sub>2</sub>, respectively) into hollow spheres with a two-layer shell structure. Reproduced from [32], with permission from the publisher

The significant finding in this work was the establishment of the electrostatically driven mechanism behind self-assembly that did not depend on thiol–Au interactions.

Refining the NP vesicle formation model, Wong and coworkers developed a new model describing the formation of hollow microspheres in which polymer and NPs form spherical aggregate intermediates through particle/polymer flocculation [34]. An important finding was the establishment of a flocculation-driven mechanism of PLL-Au NP template growth, which led to a new understanding of how to control Au NP/SiO<sub>2</sub> NP hollow sphere sizes (Fig. 4). Dis-assembly of the shell was possible when the pH of the suspending fluid was made lower than the point of zero charge of SiO<sub>2</sub> (~2). The process was reversed on raising the pH.

### 2.3 Preparation of One-Nanoparticle-Type Hollow Spheres

In 2005, Rana et al. further expanded the scope of methods for forming colloidal templates in situ by devising a reaction scheme that utilized multivalent anions (such as tetrasodium ethylenediamine tetraacetate, EDTA) over previously used Au or CdSe NPs. The governing synthesis parameter is the “*R* ratio”, defined as the total negative charge from the multivalent anion divided by the total positive charge from the polymer. This new formation pathway relies on the counteranion condensation of EDTA and other multivalent anions with polyamines, to form polymer/salt

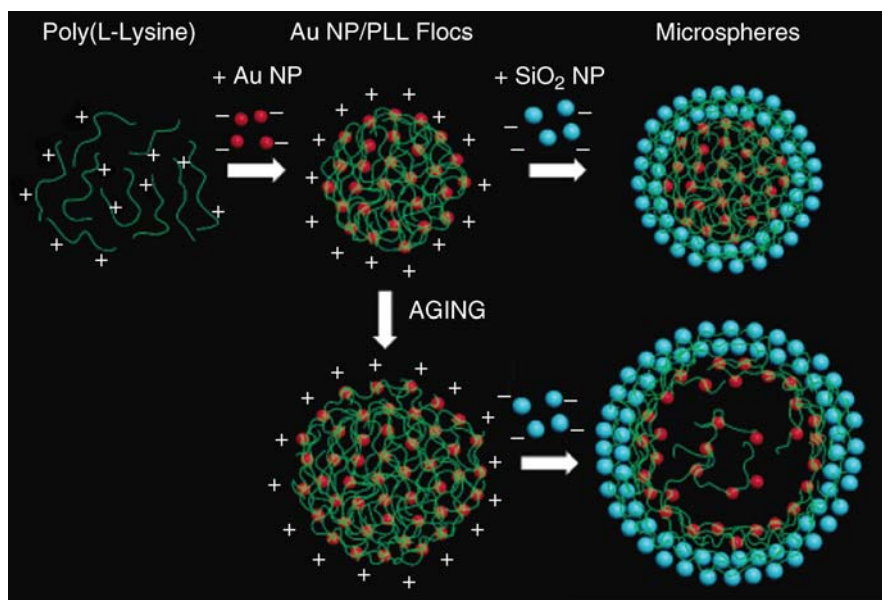


**Fig. 4** Flocculation-based self-assembly of organic-inorganic hollow spheres from PLL, Au NPs and SiO<sub>2</sub> NPs. Reproduced from [34], with permission from the publisher

aggregate colloidal templates. McKenna et al. reported similar aggregation behavior of polypeptides [85]. This salt-induced aggregation of polymer follows a very different mechanism from that in the cases of Au NP/PLL and CdSe QD/PLL. From a capsule synthesis point-of-view, salt-induced aggregation eventually yields materials composed of one NP composition whereas the other cases necessarily lead to materials composed of two NP compositions (Fig. 5).

Shell formation occurs when negatively charged SiO<sub>2</sub> NPs (at pH above its point of zero charge of 2) are contacted with the polymer/salt aggregates, such that the NPs adsorb to form a shell. Because the shell is many times thicker than the NP diameter, it has been proposed that the NPs penetrate into the polymer/salt aggregates before depositing, thereby forming a thick shell. This thick shell is responsible for the structural stability of these NACs on drying. Because the polymer/salt aggregates grow in time as metastable species (with growth rates a function of the  $R$  ratio), the capsule sizes can be controlled by both growth time and  $R$  ratio. Larger silica capsules are prepared with polymer/salt aggregates aged for longer times (30 min) rather than shorter times (3 min) (Fig. 6). The capsule material is essentially made of NPs and polymer in the shell, in which the polymer holds the oppositely charged NPs together. Interestingly, the NAC interior can contain either the polymer/salt aggregate or water, depending on the salt type used. Thus polymer-filled or water-filled capsules can be generated in one pot, merely by changing the precursor [35].

Subsequent investigations have established the general nature of the tandem assembly method using a host of linear cationic polymers [such as PLL and poly(allylamine hydrochloride), PAH] and multivalent salt variants (monosodium

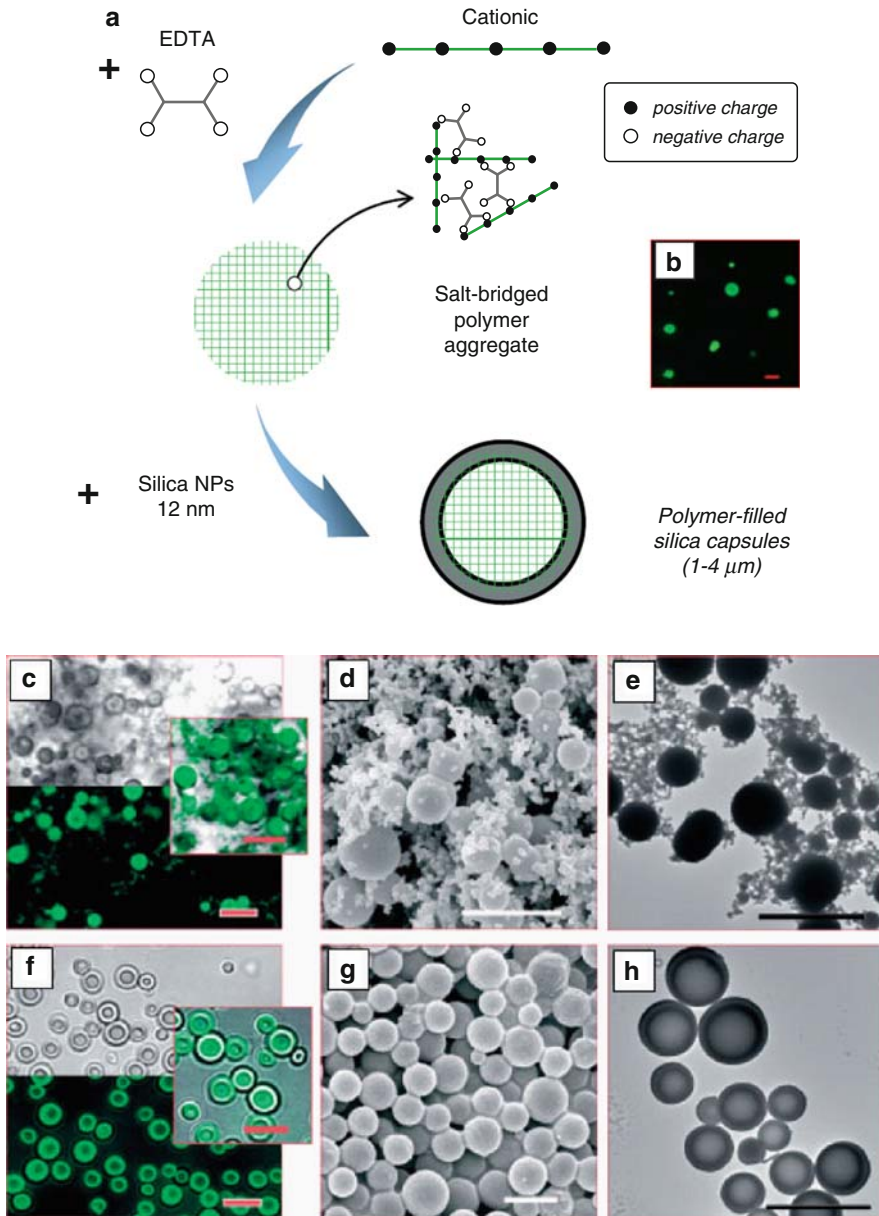
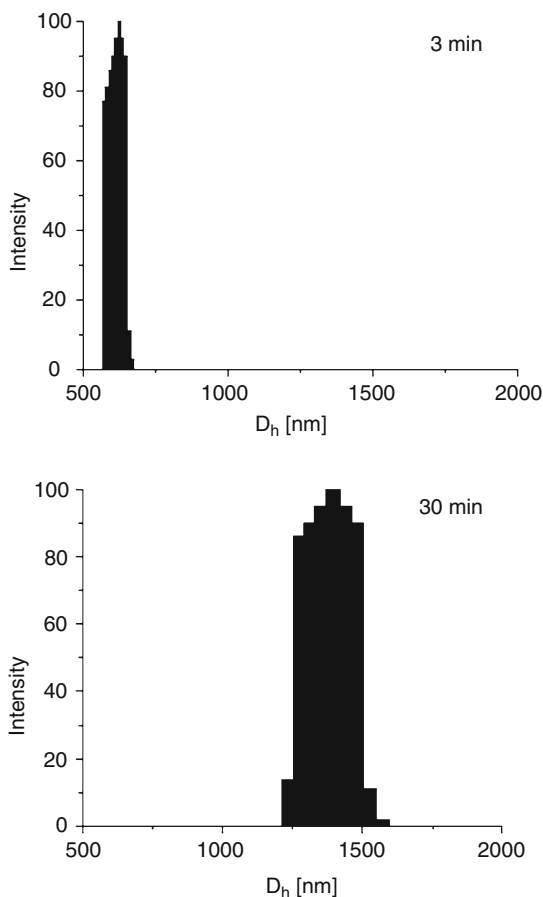


**Fig. 5** (a) Proposed schematic of the tandem self-assembly process in which positively charged polymer chains ionically cross-link with negatively charged multivalent anions, and silica nanoparticles subsequently deposit around the polymer aggregates. (b) Confocal image of EDTA-bridged PLL-FITC aggregates. (c, f) Bright field (top), confocal (bottom), and combined bright field/confocal (insets) of three different silica structures suspended in water. SEM (d, g) and TEM (e, h) images of silica structures correspond to structures in images (c and f), respectively. Scale bars: 5 μm. Reproduced from [35], with permission from the publisher

**Fig. 6** Size distribution of citrate-bridged PAH aggregates ( $R = 10$ ) after aging for 3 min (*top*) and 30 min (*bottom*). Reproduced from [35], with permission from the publisher



citrate, disodium citrate, sodium acetate, trisodium citrate, sodium succinate, EDTA, and  $\text{Na}_2\text{HPO}_4$ ). Besides  $\text{SiO}_2$  NP capsules, capsules made of  $\text{SnO}_2$  NPs, ZnO NPs,  $\text{Fe}_2\text{O}_3$  NPs,  $\text{Fe}_3\text{O}_4$  NPs, CdSe QDs, polymer,  $\text{Al}_2\text{O}_3$ - $\text{SiO}_2$  NPs, and  $\text{SiO}_2$  NPs-silicic acid have been successfully synthesized [80, 81, 86–88]. A variation of tandem assembly was reported by Tropak et al. in which nanocomposite magnetic microspheres were formed through coascervates by reacting PLL with citrate-stabilized  $\text{Fe}_2\text{O}_3$  NPs and subsequent cross-linking with glutaraldehyde [89, 90]. In more recent developments, Murthy et al. describe formation of patchy or multicompartament capsules using a blend of polymers (PAH and PLL), citric acid and  $\text{SiO}_2$  NPs [91].

The unique selling proposition of the tandem-assembly process is its contribution to the field of green chemistry in obtaining closed-shell colloidal structures through an environmentally friendly route, as the entire synthesis is carried out in water, at near neutral pH, and at room temperature. Further, the size of the colloidal template can be controlled by the charge ratios of reactants, which results in structures with sizes ranging from 100 nm to 2  $\mu\text{m}$  [32–35, 80, 81].

## 2.4 Applications and Properties of Tandem-Assembled Capsules

### 2.4.1 Optical Properties

#### Photoresponsive Delivery Systems

In the fields of medicine and drug delivery, photoresponsive delivery systems have received much attention in recent years because irradiation with light provides a direct, non-invasive method for releasing active molecules. This offers significant advantages over conventional approaches of drug delivery that rely on altering local environments (through the use of triggers such as pH, ionic strength, and temperature) to release actives, often resulting in undesired side effects. Engineered photoresponsive systems with NPs or dyes that absorb in the near-infrared (NIR) region are advantageous because most body tissues show weak light absorption, thus protecting healthy tissue while selectively treating affected tissue. In advancing photoresponsive delivery technologies, metal–NP-shelled hollow spheres from tandem assembly can be engineered to provide suitable candidates [66].

One of the key features of tandem assembly is the ability to encapsulate compounds easily and without damage. In a demonstration of applications of optically functional NACs for medical applications, Yu et al. synthesized NIR NACs, where an FDA-approved photosensitizer dye called indocyanine green (ICG) was successfully incorporated into silica/polymer capsules with diameters ranging from 0.6 to 1.0  $\mu\text{m}$ . ICG loading was readily controlled, with a maximum attained loading of  $\sim 23$  wt%. Leakage tests carried out for over 24 h at room temperature indicated negligible ICG leakage in a phosphate buffer saline solution that demonstrated the robust nature of NACs. However, ICG-containing capsules were active (capable of heat generation) to NIR laser-induced irradiation and were stable to multiple photothermal heating cycles. Fibroblast cells exposed to these capsules remained viable even after 2 days of incubation, thus these NACs serve as a promising material for photothermal therapy, offering cost and processing advantages over LBL and reduction-reaction-based Au-NP capsules and Au-nanoshells (Fig. 7) [86].

#### Optical Stability and Targeted Fluorescence Imaging

ICG finds applications as a fluorescent probe in clinical imaging. Challenges to realizing ICG as a probe for targeted fluorescence imaging in vivo emerge from its optical instability and tendency to excessively accumulate in the liver. Yaseen et al. recently devised a versatile and inexpensive route to the encapsulation of ICG within NACs, and performed targeted fluorescence imaging in vivo for the first time ever. Negatively charged constructs, formed by a coating of magnetite ( $\text{Fe}_3\text{O}_4$ ) NPs and polyacrylic acid (PAA), were shown to predominantly accumulate in lungs, whereas neutrally charged capsules formed from PLL and ICG exhibited a prolonged circulation time in the bloodstream.

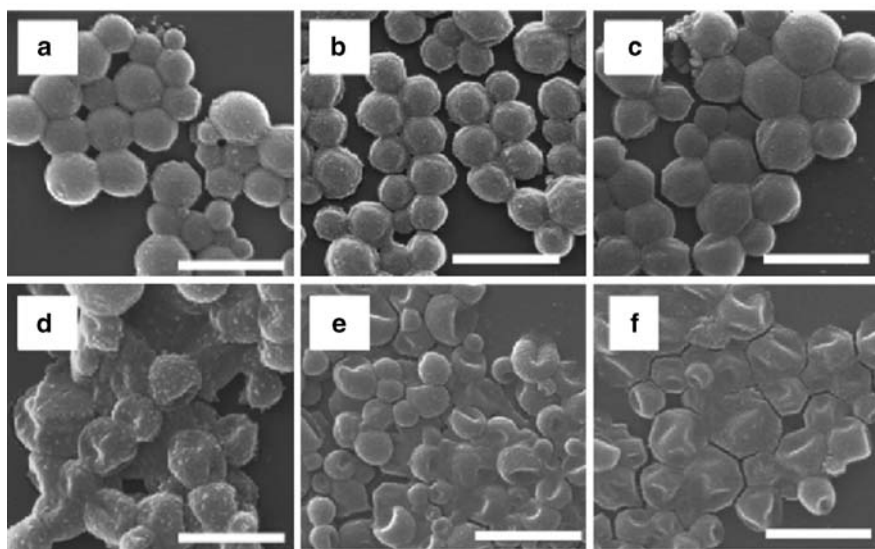
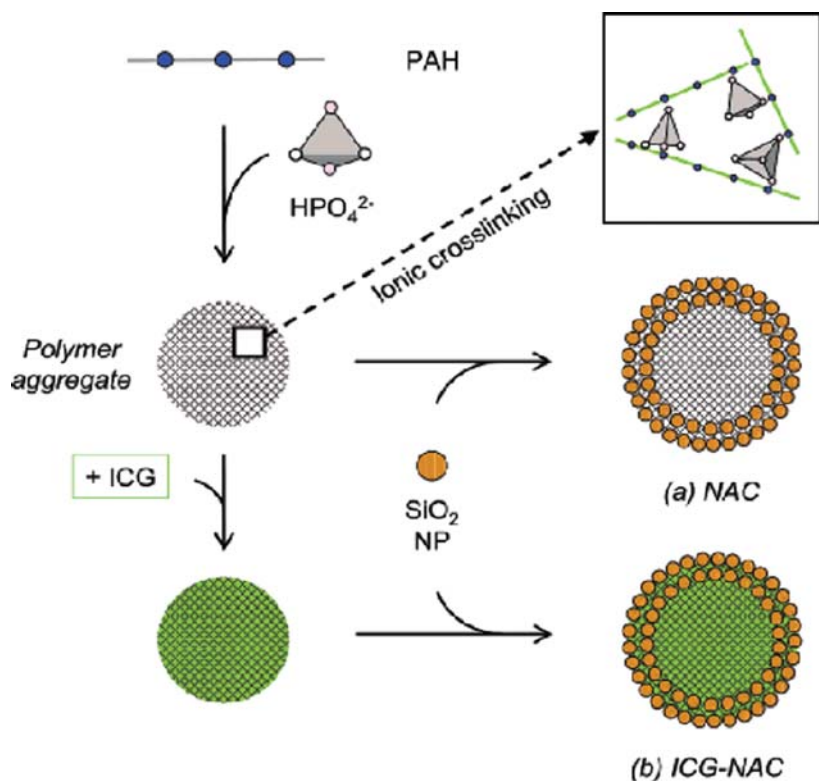


**Fig. 7** (Above) Formation mechanism of NACs and ICG-containing NACs (ICG-NACs). (Below) SEM images of ICG-NACs irradiated at different temperatures: (a) 23, (b) 40, (c) 50, (d) 60, (e) 70, (f) 73°C. Scale bars: 2 μm. Reproduced from [86], with permission from the publisher

## Optical Devices

Semiconductor NPs such as QDs have successfully been utilized for their size-dependent optical properties and find applications as optical contrast agents for biological tagging, in photovoltaics, and in lasing. In the application of QDs for optical lasing, requirements are high volume fractions of QDs, rapid optical pumping, and an optical feedback media that stimulates spontaneously emitted photons. In this regard, spherical microcavities have been established to present the ideal feedback geometry for confining the propagation of light in 3D. Cha et al. showed that hollow spheres of CdSe/CdS QDs, formed with water-soluble diblock copolypeptides and SiO<sub>2</sub> NPs, could be used for microcavity lasing applications. These spheres have a high QD volume fraction and their hollow, 3D geometry provides an ideal combination of quantum and optical confinement properties, wherein electronic states of the confined QDs are coupled to the photonic states of the spherical microcavity [84].

Another variant of semiconductor NPs uses SnO<sub>2</sub>, with applications in displays, solar cells, sensors, and photocatalysis. Assembly of SnO<sub>2</sub> NPs in a spherical shell construct is desirable in that an optically active encapsulation device can be realized. Yu et al. recently reported preparation of semiconductor SnO<sub>2</sub> NACs, using PAH polymer and Na<sub>2</sub>HPO<sub>4</sub> polyelectrolyte, that exhibited the size-dependent optical properties of the SnO<sub>2</sub> NPs building blocks. Further, the size of the resulting SnO<sub>2</sub> NACs were easily controllable by the aging time of the PAH/Na<sub>2</sub>HPO<sub>4</sub> aggregates, demonstrating flexibility in creating optical constructs of desired size. The optical properties of SnO<sub>2</sub> NACs were measured using diffuse reflectance UV-vis spectroscopy and found to be similar to SnO<sub>2</sub> NPs, suggesting their application in light-responsive encapsulation devices (Fig. 8) [81].

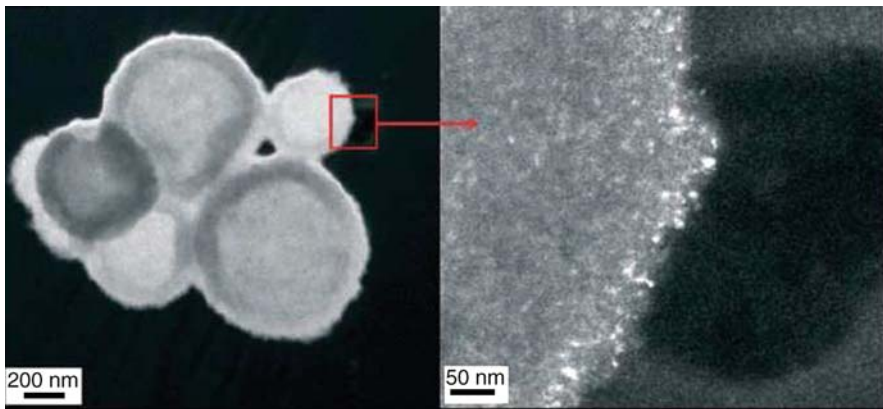


**Fig. 8** TEM image (*left*) of SnO<sub>2</sub> NACs, prepared with PAH and phosphate ions. TEM image of NAC walls (*right*) comprised of SnO<sub>2</sub> NPs. Reproduced from [81], with permission from the publisher

## 2.4.2 Mechanical Properties

The mechanical properties of microcapsules are characterized by parameters (mechanical strength, stiffness, buckling) that describe their resistance to deformation and structural change when subjected to an external load from mechanical stress or triggers such as pH, ionic strength, and temperature. Mechanical properties largely depend on the local microstructure of the capsule shell wall in terms of composition and thickness (based on its permeability or porosity), and of the core (water-filled or polymer-filled). It is useful to distinguish mechanical properties from structural stability, which in the parlance of microcapsules are changes associated with the structure of microcapsules during the drying step of synthesis. Depending on the anticipated application, structural collapse of capsules subjected to mechanical stress or triggers should either occur or be avoided.

### Encapsulation and Release Properties

Rapid and facile generation of capsules from tandem assembly in aqueous media is amenable to encapsulation of water-soluble compounds. Encapsulation of ICG dye within PAH/ $\text{H}_2\text{PO}_4$  aggregates was shown by Yu et al. Enzyme encapsulation and the feasibility of capsules to serve as reaction vessels was demonstrated by Rana et al. In their study, they encapsulated acid phosphatase enzyme in PLL–citrate–silica sols and suspended the spheres in a solution containing fluorescein diphosphate. Fluorescence increased in intensity within the shell walls as fluorescein was formed by enzymatic cleavage of phosphate groups. This study showed that microcapsules could serve as reaction vessels that allow enzymatic action to take place in a protective environment and allow for reactants and/or products to diffuse through permeable shell walls.

Bagaria et al. developed new routes for controlling shell wall thickness by adding silicic acid to NACs formed by tandem assembly of PAH, citric acid, and  $\text{SiO}_2$  NPs. Diffusion of silicic acid through  $\text{SiO}_2$  NPs resulted in an inward thickening of shells walls, confirmed by thermogravimetric analysis (TGA) and decreased dye release [88].

To describe the concentration profiles and release kinetics of fluorescein from single NP-shelled capsules, Muñoz Tavera et al. solved a mathematical model that describes unsteady-state transport from multilayered spheres using the Sturm–Liouville approach [92]. Several aspects of dye release, such as the asymptotic plateau effect of diffusive release and the effects of capsule diameter and shell thickness distribution on dye release, were captured by the model and confirmed by experimental data.

In more recent developments, Murthy et al. report a novel variant of tandem assembly leading to the formation of patchy or multicompartiment anisotropic microspheres from NP/polymer assembly and demixing of polyamine. On sequentially mixing a blend of PLL and PAH with citric acid and a silica source, PLL/PAH solution was seen to phase-separate as heterogeneous domains. Addition of  $\text{SiO}_2$  NPs

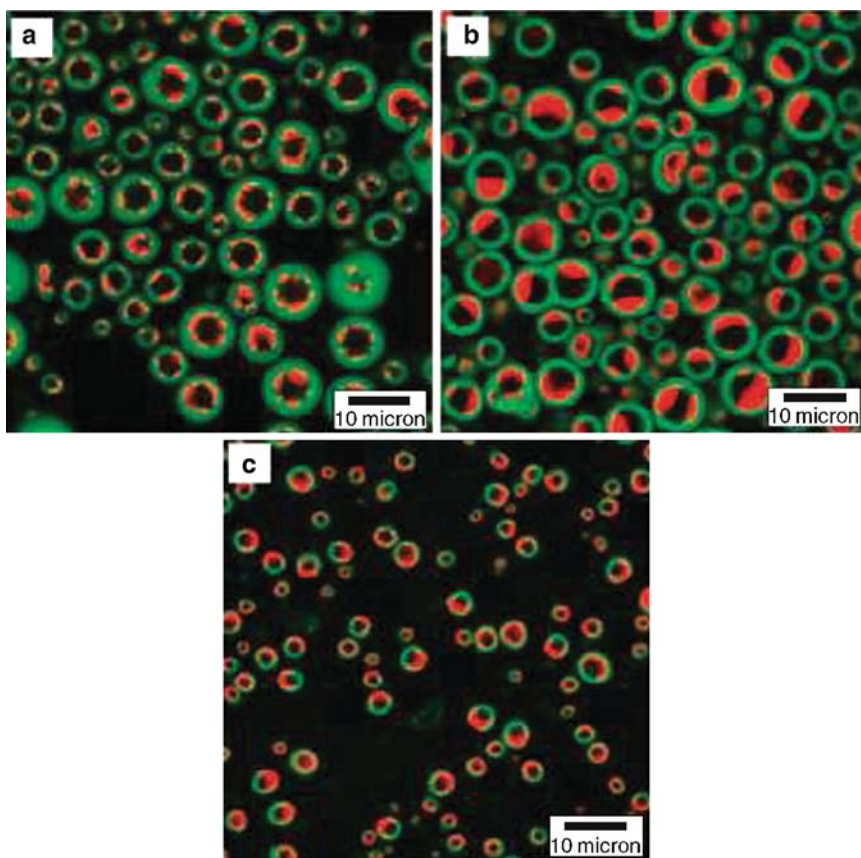


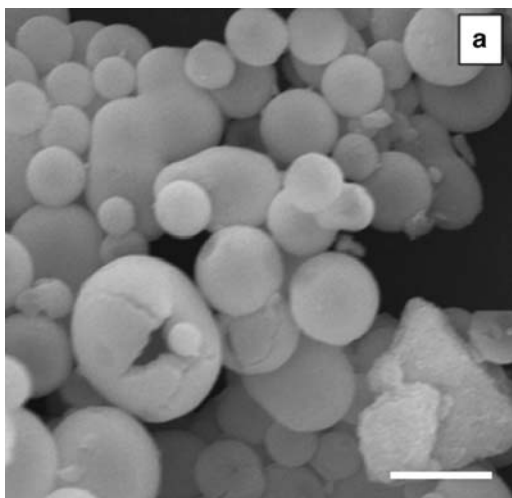
**Fig. 9** Patchy particles synthesized by stabilizing PLL-PAH/citrate aggregates with SiO<sub>2</sub> NPs at various PLL:PAH ratios: (a) 75:25, (b) 50:50, (c) 25:75. Reproduced from [91], with permission from the publisher

resulted in hollow, water-filled capsules with PAH-citrate domains attached to the cell walls. Addition of silicic acid resulted in solid spheres with PAH and PLL present in discrete domains. This method of generating compartmentalized microspheres promises to hold great potential for targeted delivery and triggered chemical release applications (Fig. 9) [91].

### Catalytic Properties

Kadali et al. demonstrated another useful application of NACs prepared by tandem assembly in the formation of catalyst support materials. NACs can be calcined to remove the polymer without collapsing the hollow sphere structure (Fig. 10). Such stability is more difficult to achieve with LBL-assembled capsules. On calcination,

**Fig. 10** SEM image of PAH-citrate and silica NACs calcined at 600°C while retaining structural stability. Scale bar: 5 μm. Reproduced from [87], with permission from the publisher



the specific surface area of the microcapsules was found to be at 259 m<sup>2</sup>/g, with a pore size of 4 nm and pore volume of 0.38 cm<sup>3</sup>/g. The surface area was similar to that of dried, calcined NPs but the porosity and pore volume were found to be significantly higher. These are useful attributes for a catalyst support. Since the material is aluminosilicate in composition, these capsules could also have applications as an acid catalyst [87].

### 3 Interfacial Stabilization and Other Approaches to the Assembly of Nanoparticle-Shelled Hollow Structures as Emulsions and Foams

The previous sections reviewed recent advancements in sequential electrostatic assembly to form NP-shelled structures. An alternate route to NP assembly arises from interfacial activity and stabilization of NPs. Colloidal particles with partial hydrophilic and hydrophobic character are known to behave like surface-active molecules (surfactants), particularly when adsorbed to a fluid–fluid interface. The assembly of small particles at interfaces is of relevance to advance fields that traditionally feature emulsions, foams, and flotation systems. It is also of pertinence to the development of new fields such as the synthesis of novel materials that include Janus particles, colloidosomes, porous solids, and anisotropic particles, all recently prepared by particle assembly at interfaces [36, 38].

Finely divided solid particles have been known since the turn of the last century to act as stabilizers in emulsions. In a seminal paper, Pickering reported that particles that preferentially wetted water over oil formed oil-in-water (O/W) emulsions through assembly at the interface [93]. This idea has been extended to the

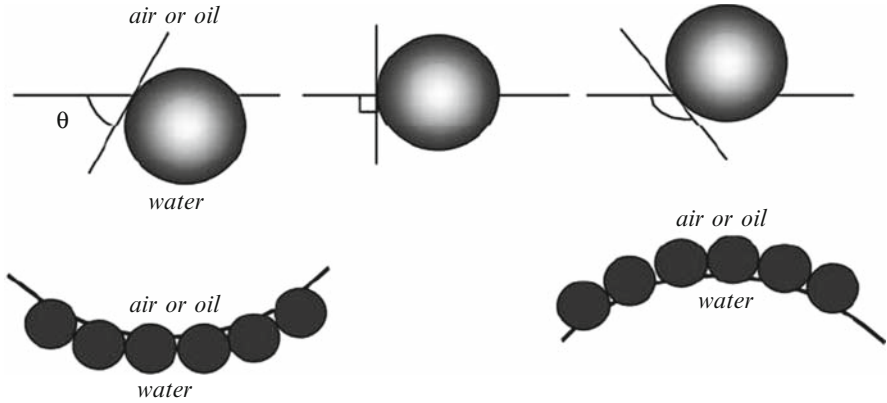


**Fig. 11** (Top) Position of a spherical (colloidal) particle at a planar fluid–water interface for a contact angle ( $\theta$ , measured through the aqueous phase)  $<90^\circ$  (left),  $90^\circ$  (center), and  $>90^\circ$  (right). (Bottom) Corresponding probable positioning of particles at a curved fluid–water interface. For  $\theta < 90^\circ$ , solid-stabilized aqueous foams or O/W emulsions may form (left). For  $\theta > 90^\circ$ , solid-stabilized aerosols or W/O emulsions may form (right). Reproduced from [37], with permission from the publisher

assembly of NPs at interfaces. There exist analogies between the interfacial assembly of colloidal particles and NPs with surfactants, in terms of their water- or oil-liking tendencies, wherein their behavior can be described in terms of wettability. This is defined by the contact angle ( $\theta$ ) formed at the fluid–fluid interface (Fig. 11). The result of this wetting behavior is the formation of either O/W or W/O emulsions with interfaces decorated by particles.

NPs, like surfactants, can facilitate phase transformation of emulsions from O/W to W/O type through change in surface wettability by altering field variables such as pH or electrolyte concentration. There are, however, important differences between stabilization of interfaces by surfactants and by particles, particularly in terms of emulsion stability. Binks has provided a comprehensive review highlighting the differences between surfactant- and particle-stabilized emulsions [37]. A key development in the latter has occurred through investigations of NP assembly at liquid–liquid interfaces, where emulsions have remarkably different properties to those formed using micron-sized particles [94]. The stability of emulsions prepared by particles is dependent on the ability of the particle to partially wet both fluid phases and to exist as a weakly flocculated state. In this regard, the energy of attachment ( $E$ ) of a particle to an interface is given by:

$$E = \pi r^2 \gamma_{\alpha\beta} (1 \pm \cos \theta)^2 \quad (1)$$

where  $r$  is the radius of the particle,  $\gamma_{\alpha\beta}$  is the interfacial tension between phases  $\alpha$  and  $\beta$ , and  $\theta$  is the contact angle of the particle defined with respect to one of the phases as the reference. It can be seen that  $E$  varies as the square of radius;

hence, NPs readily stabilize interfaces, assuming favorable wetting conditions (favorable  $\theta$ ). In contrast, micron-sized particles have to overcome an initially high energetic penalty arising from steric factors. However, once formed, the emulsions obtained are highly stable because  $E$  well exceeds the thermal energy ( $kT$ ,  $k$  being Boltzmann's constant and  $T$  temperature), so they are not easily destabilized by thermal fluctuations. At very low size ranges ( $<10$  nm), NPs tend to behave in a manner analogous to surfactants in that thermal fluctuations facilitate easy adsorption and desorption from interfaces. Thus, an optimum NP size (10–100 nm) is suitable for formation of stable emulsions [37].

Stability of NP-assembled emulsions can be controlled further in the presence of surfactants. Binks and coworkers report synergistic benefits when negatively charged silica NPs and cationic surfactants, or positively charged silica NPs and anionic surfactants, were used to create O/W emulsions. These emulsions demonstrated high kinetic stability to creaming and coalescence, due to synergistic lowering of interfacial tension by surfactants and of wetting behavior by NPs [94, 95]. The stability of emulsions prepared using NPs and uncharged nonionic surfactants was seen to be strongly dependent on the protocol of preparation, where the absence of electrostatic interactions between NPs and surfactants resulted in scenarios in which either interfacial tension or wettability effects dominated, thus resulting in unstable or stable emulsions, respectively [94, 96].

Binks and Murakami report unique phase transformation behavior in NP-induced phase transformation in particle-stabilized air–water systems that is not demonstrated by surfactants. It was seen that by altering silica-NP (20–30 nm) hydrophobicity at constant air:water ratio or by changing the air:water ratio at fixed NP wettability, phase inversion could be induced from air-in-water to water-in-air foams (Fig. 12) [36]. This investigation thus demonstrates that control over interfacial assembly of NPs leads to the formation of stable NP-shelled hollow spheres, thus resulting in the formation of stable foams, dispersions, and powders with far reaching consequences in opening new avenues for advanced encapsulation (Fig. 13).

In other unique structures that emerge from interfacial NP assembly, Weitz and coworkers report formation of solid capsules with precise size control over permeability and mechanical strength through self-assembly of 0.9- $\mu$ m colloidal particles at the interface of emulsion droplets. Particles are locked to form elastic shells and then transferred to a continuous-phase fluid that is of similar composition to the fluid inside the droplets, resulting in colloidosomes with characteristics of high structural robustness [38, 40]. Duan et al. report interfacial assembly of magnetic NPs and formation of water-dispersible NP colloidosomes with permeable shells, while He and Yu report formation of silica NP-armored polyaniline microspheres in particle-stabilized emulsions [97, 98]. In all such cases, the driving force for assembly at interfaces is stabilization through minimization of exposed interfacial area [36, 37, 39, 40, 53, 57, 58, 73, 94–96, 98–110].

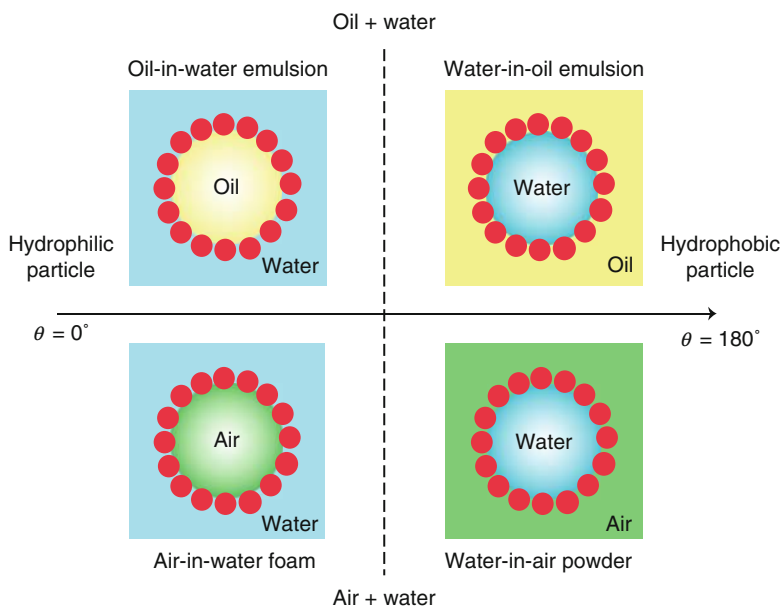


**Fig. 12** Dispersed systems prepared from fluid mixtures and colloidal particles/nanoparticles. For oil–water mixtures (*top*), emulsion drops of O/W emulsions and W/O emulsions are stabilized with hydrophilic or hydrophobic particles, respectively. For air–water mixtures (*bottom*), air-in-water foams or water-in-air powders can be likewise stabilized through the use of nanoparticles. Reproduced from [36], with permission from the publisher

## 4 Conclusions and Future Work

This chapter describes the non-LBL approaches of tandem assembly and interfacial stabilization for the formation of closed shell structures, with an emphasis on ensembles in which NPs constitute the shell. Tandem assembly is a versatile and environmentally friendly route to the formation of useful NP-shelled capsules. In contrast to sacrificial core templating and LBL assembly methods, tandem assembly has the important differentiating feature that it avoids the incineration or solvent dissolution step to generate the hollow interior of the capsule. Enhancements in optical, mechanical, catalytic, and release properties of such materials hold great promise for their application in photoresponsive delivery systems, catalysis, and encapsulation. Interfacial stabilization routes are found to yield NP-shelled structures in the form of emulsions and foams that have enhanced stability over those from conventional, surfactant-based approaches. Unusual interactions of the NP with fluid interfaces have made possible new structures, such as water-in-air foams, colloidosomes, and anisotropic particles.

As a future direction of research, capsule walls comprised of amphiphilic NPs (Janus capsules) could give rise to a new class of material that has the dual properties of interfacial activity and targeted materials delivery. LBL assembly has previously

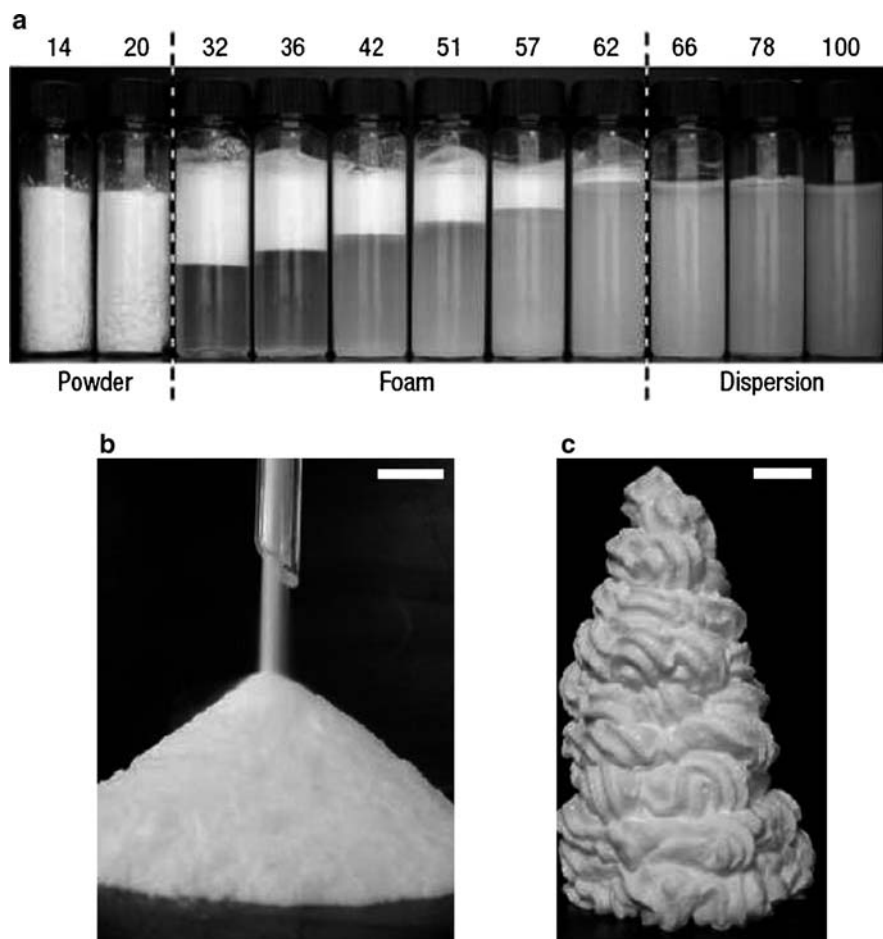


**Fig. 13** Transitional inversion of the curvature of air-water surfaces with respect to particle hydrophobicity. **(a)** Vessels containing 2 wt% (relative to water) of dichloromethylsilane-coated silica particles with fixed volume fraction of water ( $\phi_w = 0.056$ ) 2 weeks after mixing and aeration, for particles of different wettability. The % SiOH content on particle surfaces (given along the top) decreases from right to left as particles become more hydrophobic; the mixtures change from aqueous dispersions to air-in-water foams (with drained water) to water-in-air powders. Inversion occurs on moving either side of the *left dashed line*. **(b)** Free-flowing powder passing through a glass funnel made by aerating 5 g of silica particles possessing 20% SiOH and 95 g of water ( $\phi_w = 0.056$ ). **(c)** Foam extruded through a serrated metal nozzle prepared by aerating 5 g of silica particles possessing 32% SiOH and 95 g of water ( $\phi_w = 0.056$ ). *Scale bars: 1 cm.* Reproduced from [36], with permission from the publisher

been used to make hollow Janus structures with amphiphilic submicron particles, and tandem assembly has until recently resulted in 1- or 2-NP-shelled capsules. This approach could be revisited wherein NPs with differing levels of hydrophilic or hydrophobic nature (such as silica NPs) could be deposited at precise locations

on templates to create Janus capsules [31, 111–113]. The use of biological hollow particles called “vaults” (~40–70 nm) could be incorporated into tandem assembly chemistry to generate multifunctional microcapsules comprised of biocompatible nanocapsules [114]. Continued development in top-down approaches of microfabrication (such as lithography and reactive-ion etching) could provide novel avenues for assembly of NP-shelled capsules into well-defined patterned macrostructured films [108].

**Acknowledgement** We acknowledge the financial support of National Science Foundation (CBET-0652073) and the Rice University Institute of Biosciences and Bioengineering Medical Innovations Award.

## References

1. Evans DF, Wennerström H (1999) *The colloidal domain: where physics, chemistry, biology and technology meet*, 2 edn. Wiley, New York
2. Israelachvili JN (1991) *Intermolecular and surface forces*. Academic, New York
3. Claesson PM, Ederth T, Bergeron V et al (1996) Techniques for measuring surface forces. *Adv Colloid Interface Sci* 67:119–183
4. Grabar KC, Brown KR, Keating CD et al (1997) Nanoscale characterization of gold colloid monolayers: a comparison of four techniques. *Anal Chem* 69(3):471–477
5. Schatz GC (2007) Using theory and computation to model nanoscale properties. *Proc Natl Acad Sci* 104(17):6885–6892
6. Tang ZY, Kotov NA (2005) One-dimensional assemblies of nanoparticles: preparation, properties, and promise. *Adv Mater* 17(8):951–962
7. Shipway AN, Katz E, Willner I (2000) Nanoparticle arrays on surfaces for electronic, optical, and sensor applications. *Chem Phys Chem* 1(1):18–52
8. Caruso F (2003) Nanoscale surface modification via sequential electrostatic assembly. In: Caruso F (ed) *Colloids and colloid assemblies*. Wiley, Weinheim
9. Parviz BA, Ryan D, Whitesides GM (2003) Using self-assembly for the fabrication of nanoscale electronic and photonic devices. *IEEE Trans Adv Packaging* 26(3):233–241
10. Chane-Ching JY, Cobo F, Aubert D et al (2005) A general method for the synthesis of nanostructured large-surface-area materials through the self-assembly of functionalized nanoparticles. *Chem Eur J* 1(3):979–987
11. Huang MH, Mao S, Feick H et al (2001) Room-temperature ultraviolet nanowire nanolasers. *Science* 292(5523):1897–1899
12. Han MY, Gao XH, Su JZ et al (2001) Quantum-dot-tagged microbeads for multiplexed optical coding of biomolecules. *Nat Biotechnol* 19(7):631–635
13. Caruso F (2001) Nanoengineering of particle surfaces. *Adv Mater* 13(1):11–22
14. Connolly S, Fitzmaurice D (1999) Programmed assembly of gold nanocrystals in aqueous solution. *Adv Mater* 11(14):1202–1205
15. Bruchez M, Moronne M, Gin P et al (1998) Semiconductor nanocrystals as fluorescent biological labels. *Science* 281(5385):2013–2016
16. Chan WCW, Nie SM (1998) Quantum dot bioconjugates for ultrasensitive nonisotopic detection. *Science* 281(5385):2016–2018
17. Alivisatos AP, Johnsson KP, Peng XG et al (1996) Organization of ‘nanocrystal molecules’ using DNA. *Nature* 382(6592):609–611
18. Mirkin CA, Letsinger RL, Mucic RC et al (1996) A DNA-based method for rationally assembling nanoparticles into macroscopic materials. *Nature* 382(6592):607–609

19. El-Sayed MA (2001) Some interesting properties of metals confined in time and nanometer space of different shapes. *Acc Chem Res* 34(4):257–264
20. Grieve K, Mulvaney P, Grieser F (2000) Synthesis and electronic properties of semiconductor nanoparticles/quantum dots. *Curr Opin Colloid Interface Sci* 5(1–2):168–172
21. Wilcox DL Sr, Berg M, Bernat T et al (1995) Hollow and solid spheres and microspheres: science and technology associated with their fabrication and application. Materials Research Society, Pittsburgh, PA
22. Yang M, Ma J, Zhang CL et al (2005) General synthetic route toward functional hollow spheres with double-shelled structures. *Angew Chem Int Ed.* 44(41):6727–6730
23. Huie JC (2003) Guided molecular self-assembly: a review of recent efforts. *Smart Mater Struct* 12(2):264–271
24. Boncheva M, Bruzewicz DA, Whitesides GM (2003) Millimeter-scale self-assembly and its applications. *Pure Appl Chem* 75(5):621–630
25. Iler RK (1966) Multilayers of colloidal particles. *J Colloid Sci* 21(6):569–594
26. Caruso RA, Antonietti M (2001) Sol-gel nanocoating: an approach to the preparation of structured materials. *Chem Mater* 13(10):3272–3282
27. Decher G, Hong JD (1991) Buildup of ultrathin multilayer films by a self-assembly process. 1. Consecutive adsorption of anionic and cationic bipolar amphiphiles on charged surfaces. *Makromol Chem Macromol Sym* 46:321–327
28. Decher G (1997) Fuzzy nanoassemblies: toward layered polymeric multicomposites. *Science* 277(5330):1232–1237
29. Caruso F, Caruso RA, Mohwald H (1998) Nanoengineering of inorganic and hybrid hollow spheres by colloidal templating. *Science* 282(5391):1111–1114
30. Caruso F (2000) Hollow capsule processing through colloidal templating and self-assembly. *Chem Eur J* 6(3):413–419
31. Jiang CY, Tsukruk VV (2006) Freestanding nanostructures via layer-by-layer assembly. *Adv Mater* 18(7):829–840
32. Wong MS, Cha JN, Choi KS et al (2002) Assembly of nanoparticles into hollow spheres using block copolypeptides. *Nano Lett* 2(6):583–587
33. Cha JN, Birkedal H, Euliss LE et al (2003) Spontaneous formation of nanoparticle vesicles from homopolymer polyelectrolytes. *J Am Chem Soc* 125(27):8285–8289
34. Murthy VS, Cha JN, Stucky GD et al (2004) Charge-driven flocculation of poly(l-lysine)-gold nanoparticle assemblies leading to hollow microspheres. *J Am Chem Soc* 126(16):5292–5299
35. Rana RK, Murthy VS, Yu J et al (2005) Nanoparticle self-assembly of hierarchically ordered microcapsule structures. *Adv Mater* 17(9):1145–1150
36. Binks BP, Murakami R (2006) Phase inversion of particle-stabilized materials from foams to dry water. *Nat Mater* 5(11):865–869
37. Binks BP (2002) Particles as surfactants - similarities and differences. *Curr Opin Colloid Interface Sci* 7(1–2):21–41
38. Dinsmore AD, Hsu MF, Nikolaidis MG et al (2002) Colloidosomes: selectively permeable capsules composed of colloidal particles. *Science* 298(5595):1006–1009
39. Horozov TS, Binks BP (2006) Particle-stabilized emulsions: a bilayer or a bridging monolayer? *Angew Chem Int Ed.* 45(5):773–776
40. Hsu MF, Nikolaidis MG, Dinsmore AD et al (2005) Self-assembled shells composed of colloidal particles: fabrication and characterization. *Langmuir* 21(7):2963–2970
41. Johnston APR, Cortez C, Angelatos AS et al (2006) Layer-by-layer engineered capsules and their applications. *Curr Opin Colloid Interface Sci* 11(4):203–209
42. Gibbs BF, Kermasha S, Alli I et al (1999) Encapsulation in the food industry: a review. *Int J Food Sci Nutr* 50(3):213–224
43. Park J, Fouche LD, Hammond PT (2005) Multicomponent patterning of layer-by-layer assembled polyelectrolyte/nanoparticle composite thin films with controlled alignment. *Adv Mat* 17(21):2575–2579
44. Nikolic K, Murugesan M, Forshaw M et al (2007) Self-assembly of nanoparticles on the surface of ionic crystals: structural properties. *Surf Sci* 601(13):2730–2734

45. Davies P, Schurr GA, Meenan P et al (1998) Engineered particle surfaces. *Adv Mat* 10(15):1264–1270
46. Niemeyer CM (2001) Nanoparticles, proteins, and nucleic acids: biotechnology meets materials science. *Angew Chem Int Ed* 40(22):4128–4158
47. Davis SA, Breulmann M, Rhodes KH et al (2001) Template-directed assembly using nanoparticle building blocks: a nanotectonic approach to organized materials. *Chem Mater* 13(10):3218–3226
48. Huwiler C, Halter M, Rezwan K et al (2005) Self-assembly of functionalized spherical nanoparticles on chemically patterned microstructures. *Nanotechnology* 16(12):3045–3052
49. Maury PA, Reinhoudt DN, Huskens J (2008) Assembly of nanoparticles on patterned surfaces by noncovalent interactions. *Curr Opin Colloid Interface Sci* 13(1–2):74–80
50. Jana NR (2004) Shape effect in nanoparticle self-assembly. *Angew Chem Int Ed* 43(12):1536–1540
51. Bognolo G (2003) The use of surface-active agents in the preparation and assembly of quantum-sized nanoparticles. *Adv Colloid Interface Sci* 106:169–181
52. Barrero A, Loscertales IG (2007) Micro- and nanoparticles via capillary flows. *Annu Rev Fluid Mech* 39:89–106
53. Hua F, Shi J, Lvov Y et al (2002) Patterning of layer-by-layer self-assembled multiple types of nanoparticle thin films by lithographic technique. *Nano Lett* 2(11):1219–1222
54. Gao JH, Zhang B, Zhang XX et al (2006) Magnetic-dipolar-interaction-induced self-assembly affords wires of hollow nanocrystals of cobalt selenide. *Angew Chem Int Ed.* 45(8):1220–1223
55. Sayle DC, Feng XD, Ding Y et al (2007) “Simulating synthesis”: ceria nanosphere self-assembly into nanorods and framework architectures. *J Am Chem Soc* 129(25):7924–7935
56. Shi ZT, Pan DY, Zhao SF et al (2006) Self-assembly of ordered silver nanoparticle chains on triblock copolymer templates. *Mod Phys Lett B* 20(20):1261–1266
57. Govor LV, Reiter G, Parisi J et al (2004) Self-assembled nanoparticle deposits formed at the contact line of evaporating micrometer-size droplets. *Phys Rev E* 69(6):061609
58. Govor LV, Reiter G, Bauer GH et al (2004) Nanoparticle ring formation in evaporating micron-size droplets. *Appl Phys Lett* 84(23):4774–4776
59. Tripp SL, Dunin-Borkowski RE, Wei A (2003) Flux closure in self-assembled cobalt nanoparticle rings. *Angew Chem Int Ed* 42(45):5591–5593
60. Haryono A, Binder WH (2006) Controlled arrangement of nanoparticle arrays in block-copolymer domains. *Small* 2(5):600–611
61. Osterloh FE, Martino JS, Hiramatsu H et al (2003) Stringing up the pearls: self-assembly, optical and electronic properties of cdse- and Au-limo<sub>3</sub>se<sub>3</sub> nanoparticle-nanowire composites. *Nano Lett* 3(2):125–129
62. Osterloh FE (2006) Directional superparamagnetism and photoluminescence in clusters of magnetite and cadmium selenide nanoparticles. *Comments Inorg Chem* 27(1–2):41–59
63. Arumugam P, Xu H, Srivastava S et al (2007) ‘Bricks and mortar’ nanoparticle self-assembly using polymers. *Polym Int* 56(4):461–466
64. Kakkassery JJ, Abid JP, Carrara M (2004) Electrochemical and optical properties of two dimensional electrostatic assembly of Au nanocrystals. *Faraday Discuss* 125:157–169
65. Angelatos AS, Radt B, Caruso F (2005) Light-responsive polyelectrolyte/gold nanoparticle microcapsules. *J Phys Chem B* 109(7):3071–3076
66. Angelatos AS, Katagiri K, Caruso F (2006) Bioinspired colloidal systems via layer-by-layer assembly. *Soft Matt* 2(1):18–23
67. Dokoutchaev A, James JT, Koene SC et al (1999) Colloidal metal deposition onto functionalized polystyrene microspheres. *Chem Mater* 11(9):2389–2399
68. De Geest BG, Skirtach AG, De Beer TRM et al (2007) Stimuli-responsive multilayered hybrid nanoparticle/polyelectrolyte capsules. *Macromol Rapid Commun* 28(1):88–95
69. Efros AL, Rosen M (2000) The electronic structure of semiconductor nanocrystals. *Annu Rev Mater Sci* 30:475–521
70. Fukumori Y, Ichikawa H (2006) Nanoparticles for cancer therapy and diagnosis. *Adv Powder Technol* 17(1):1–28

71. Wang WT, Wang YM, Dai ZH et al (2007) Nonlinear optical properties of periodic gold nanoparticle arrays. *Appl Surf Sci* 253(10):4673–4676
72. Zhang H, Edwards EW, Wang DY et al (2006) Directing the self-assembly of nanocrystals beyond colloidal crystallization. *PCCP* 8(28):3288–3299
73. Barsotti RJ, Vahey MD, Wartena R et al (2007) Assembly of metal nanoparticles into nanogaps. *Small* 3(3):488–499
74. Hofman-Caris CHM (1994) Polymers at the surface of oxide nanoparticles. *New J Chem* 18(10):1087–1096
75. Caruso F (2003) Hollow inorganic capsules via colloid-templated layer-by-layer electrostatic assembly. In *Colloid Chem II*, Vol. 227, pp 145–168
76. Capsulation (2009) Turning ideas into reality. <http://www.capsulation.com/en/home.html>
77. Priest C, Quinn A, Postma A et al (2008) Microfluidic polymer multilayer adsorption on liquid crystal droplets for microcapsule synthesis. *Lab Chip* 8(12):2182–2187
78. Tjipto E, Cadwell KD, Quinn JF et al (2006) Tailoring the interfaces between nematic liquid crystal emulsions and aqueous phases via layer-by-layer assembly. *Nano Lett* 6(10):2243–2248
79. Wang Y, Angelatos AS, Caruso F (2008) Template synthesis of nanostructured materials via layer-by-layer assembly. *Chem Mater* 20(3):848–858
80. Murthy VS, Rana RK, Wong MS (2006) Nanoparticle-assembled capsule synthesis: Formation of colloidal polyamine-salt intermediates. *J Phys Chem B* 110(51):25619–25627
81. Yu J, Murthy VS, Rana RK, Wong MS (2006) Synthesis of nanoparticle-assembled tin oxide/polymer microcapsules. *Chem Commun* 10:1097–1099
82. Partch R (1997) Materials synthesis and characterization. In: Perry D (ed) Plenum, New York, pp 1–17
83. Atwood JL, Davies JED, Macnicol DD et al (1996) Templating, self assembly and self-organization. In: Sauvage JP, Hosseini MW (eds) *Comprehensive supramolecular chemistry*, Vol. 35b. Pergamon, Oxford, pp 507–528
84. Cha JN, Bartl MH, Wong MS et al (2003) Microcavity lasing from block peptide hierarchically assembled quantum dot spherical resonators. *Nano Lett* 3(7):907–911
85. McKenna BJ, Birkedal H, Bartl MH et al (2004) Micrometer-sized spherical assemblies of polypeptides and small molecules by acid-base chemistry. *Angew Chem Int Ed* 43(42):5652–5655
86. Yu J, Yaseen MA, Anvari B, Wong MS (2007) Synthesis of near-infrared-absorbing nanoparticle-assembled capsules. *Chem Mater* 19(6):1277–1284
87. Kadali SB, Soutanidis N, Wong MS (2008) Assembling colloidal silica into porous hollow microspheres. *Top Catal* 49:251–258
88. Bagaria HG, Kadali SB, Wong MS (2009) Shell thickness control of nanoparticle/polymer composite microcapsules (unpublished)
89. Toprak MS, McKenna BJ, Mikhaylova M et al (2007) Spontaneous assembly of magnetic microspheres. *Adv Mater* 19(10):1362–1368
90. Toprak MS, McKenna BJ, Waite JH et al (2007) Control of size and permeability of nanocomposite microspheres. *Chem Mater* 19(17):4263–4269
91. Murthy VS, Kadali SB, Wong MS (2009) Polyamine-guided synthesis of anisotropic, multi-compartment microparticles. *ACS Appl Mat Interfaces* 1(3):590–596
92. Tavera EM, Kadali SB, Bagaria HG et al (2009) Experimental and modeling analysis of diffusive release from single-shell microcapsules. *AIChE J* 55(11):2950–2965
93. Pickering SU (1907) Emulsions. *J Chem Soc* 91:2001–2021
94. Binks BP, Whitty CP (2005) Nanoparticle silica-stabilized oil-in-water emulsions: improving emulsion stability. *Colloids Surf A* 253(1–3):105–115
95. Binks BP, Rodrigues JA, Frith WJ (2007) Synergistic interaction in emulsions stabilized by a mixture of silica nanoparticles and cationic surfactant. *Langmuir* 23(7):3626–3636
96. Binks BP, Desforges A, Duff DG (2007) Synergistic stabilization of emulsions by a mixture of surface-active nanoparticles and surfactant. *Langmuir* 23(3):1098–1106
97. Duan HW, Wang DY, Sobal NS et al (2005) Magnetic colloidosomes derived from nanoparticle interfacial self-assembly. *Nano Lett* 5(5):949–952

98. He YJ, Yu XY (2007) Preparation of silica nanoparticle-armored polyaniline microspheres in a Pickering emulsion. *Mater Lett* 61(10):2071–2074
99. Binks BP, Clint JH, Fletcher PDI et al (2006) Growth of gold nanoparticle films driven by the coalescence of particle-stabilized emulsion drops. *Langmuir* 22(9):4100–4103
100. Binks BP, Duncumb B, Murakami R (2007) Effect of pH and salt concentration on the phase inversion of particle-stabilized foams. *Langmuir* 23(18):9143–9146
101. Binks BP, Kirkland M (2002) Interfacial structure of solid-stabilized emulsions studied by scanning electron microscopy. *PCCP* 4(15):3727–3733
102. Binks BP, Rodrigues JA (2007) Double inversion of emulsions by using nanoparticles and a di-chain surfactant. *Angew Chem Int Ed* 46(28):5389–5392
103. Binks BP, Rodrigues JA (2007) Enhanced stabilization of emulsions due to surfactant-induced nanoparticle flocculation. *Langmuir* 23(14):7436–7439
104. Nie YR, Li W, An LJ et al (2006) Fabricating ordered 2D arrays of magnetic rings on patterned self-assembly monolayers via dewetting and thermal decomposition. *Colloids Surf A* 278(1–3):229–234
105. Schacht S, Huo Q, VoigtMartin IG et al (1996) Oil-water interface templating of mesoporous macroscale structures. *Science* 273(5276):768–771
106. Madou M (1998) *Fundamentals of microfabrication*. CRC, Boca Raton
107. Cui TH, Hua F, Lvov Y (2004) Lithographic approach to pattern multiple nanoparticle thin films prepared by layer-by-layer self-assembly for microsystems. *Sens Actuators A* 14(2–3): 501–504
108. Choi DG, Jang SG, Kim S et al (2006) Multifaceted and nanobored particle arrays sculpted using colloidal lithography. *Adv Funct Mater* 16(1):33–40
109. Barry CR, Lwin NZ, Zheng W et al (2003) Printing nanoparticle building blocks from the gas phase using nanoxerography. *Appl Phys Lett* 83(26):5527–5529
110. Barry CR, Steward MG, Lwin NZ et al (2003) Printing nanoparticles from the liquid and gas phases using nanoxerography. *Nanotechnology* 14(10):1057–1063
111. Zharov VP, Galitovskaya EN, Johnson C et al (2005) Synergistic enhancement of selective nanophotothermolysis with gold nanoclusters: potential for cancer therapy. *Laser Surg Med* 37(3):219–226
112. Choi WS, Koo HY, Park JH et al (2005) Synthesis of two types of nanoparticles in poly-electrolyte capsule nanoreactors and their dual functionality. *J Am Chem Soc* 127(46): 16136–16142
113. Perro A, Reculosa S, Ravaine S et al (2005) Design and synthesis of Janus micro and nanoparticles. *J Mater Chem* 15(35–36):3745–3760
114. Kickhoefer VA, Garcia Y, Mikyas Y et al (2005) Engineering of vault nanocapsules with enzymatic and fluorescent properties. *Proc Natl Acad Sci* 102(12):4348–4352